

# Molecular imaging and therapeutic efficacy of $^{188}\text{Re}$ -(DXR)-liposome-BBN in AR42J pancreatic tumor-bearing mice

YA-JEN CHANG, CHIA-YU YU, CHIN-WEI HSU, WAN-CHI LEE,  
SU-JUNG CHEN, CHIH-HSIEN CHANG and TE-WEI LEE

Institute of Nuclear Energy Research, No. 1000 Wenhua Rd., Jiaan Village,  
Longtan Township, Taoyuan County 32546, Taiwan, R.O.C.

Received April 3, 2012; Accepted May 28, 2012

DOI: 10.3892/or.2012.1978

**Abstract.** Liposomes are good candidates as drug carriers and have been widely investigated in drug delivery systems. In this study, a new combination of bimodal  $^{188}\text{Re}$ -(DXR)-liposome-BBN radiochemotherapeutics was designed and studied for treating solid pancreatic tumor by intravenous administration. The *in vivo* nuclear microSPECT/CT imaging of tumor targeting, prolonged survival time and therapeutic efficacy were evaluated in AR42J malignant pancreatic solid tumor-bearing nude mice. MicroSPECT/CT imaging of  $^{188}\text{Re}$ -liposome-BBN pointed to significant targeting in tumors at 24 h after intravenous injection ( $\text{SUV}=2.13\pm0.98$ ). Co-injection of a blocking dose of cold BBN (4 mg/kg) inhibited the accumulation of  $^{188}\text{Re}$ -liposome-BBN in tumors ( $\text{SUV}=1.82\pm0.31$ ). For therapeutic efficacy, inhibition of tumor growth in mice treated with  $^{188}\text{Re}$ -DXR-liposome-BBN was precisely controlled [mean growth inhibition rate ( $\text{MGI}$ ) = 0.092] and had longer survival time [life-span ( $\text{LS}$ ) = 86.96%] than those treated with anticancer drug  $^{188}\text{Re}$ -liposome-BBN ( $\text{MGI}$  = 0.130;  $\text{LS}$  = 75%), Lipo-Dox-BBN ( $\text{MGI}$  = 0.666;  $\text{LS}$  = 3.61%) and untreated control mice. An additive tumor regression effect was observed ( $\text{CI}$  0.946) for co-delivery of  $^{188}\text{Re}$ -DXR-liposome-BBN radiochemotherapeutics. These results point to the potential benefit of the  $^{188}\text{Re}$ -(DXR)-liposome-BBN radiochemotherapeutics for adjuvant cancer treatment with applications in oncology.

## Introduction

The development of ligand-targeted therapeutics in anticancer therapy has gained momentum in recent years (1). Systemic cytotoxic chemotherapy shows little selectivity and side effects. One strategy to improve the lack of selectivity is to couple therapeutics to antibodies or smaller molecule peptides (2). Among

the most relevant peptide receptors, the bombesin receptors are of major interest, because they were found to be overexpressed in various cancers such as prostate (3,4), breast (5,6), and small cell lung cancer (7). The human counterparts of bombesin, namely gastrin-releasing peptide (8,9) and neuromedin B (8), have been found in mammalian tissue. Gastrin-releasing peptide receptors (GRPR) are overexpressed on a variety of human tumors such as prostate, breast, and lung cancer. Bombesin (BBN) is a 14 amino acid peptide with high affinity for these GRPRs. Bombesin and gastrin-releasing peptide (GRP) are potent neuropeptides expressed by prostate cancer neuroendocrine cells and are related to the progression of this malignancy.

Nanoliposomes are double-membrane lipid vesicles capable of packaging drugs for various delivery applications (10). Nano-pegylated liposomes can evade the reticuloendothelial system and remain in the circulation for prolonged periods, improving tumor targeting and efficacy in animal models (11,12). Nano-pegylated liposomes provide passive targeting because nanoliposome accumulation in tumors is by means of the enhanced permeability and retention (EPR) effect through leaky tumor vasculature (12). Preclinical studies have shown that cytotoxic agents entrapped in pegylated liposomes tend to accumulate in tumors (13,14).

Preclinical studies of tumor therapy with radionuclide-liposome conjugates or liposome-mediated radiotherapeutics have been reported (15-18). Rhenium- $^{188}$  is a radionuclide used for imaging and therapeutic dual applications due to its short physical half-life of 16.9 h with 155 keV gamma emissions for imaging, and its 2.12 MeV  $\beta$  emission with maximum tissue penetration range of 11 mm for tumor therapeutics (19). In addition,  $^{188}\text{Re}$  can be obtained from a commercial nuclear generator, which makes it convenient for routine research and clinical use.

Chemoradiotherapy is a standard treatment for patients with locally advanced rectal cancer. Direct targeted therapy approaches target tumor antigens to change signalling by monoclonal antibodies, peptide or small molecule drugs. Drugs can actively target tumors using tumor-specific antibody or peptide ligands binding to receptors that are present on tumor cells. In this study, a new combination of peptide targeted radiochemo-therapeutics was designed and studied for treating solid tumors of the pancreas by intravenous administration. The *in vivo* nuclear images of tumor, prolonged survival time and therapeutic efficacy of radiochemotherapeutics of  $^{188}\text{Re}$ -(DXR)-liposome-BBN were evaluated in AR42J malignant pancreas solid tumor-bearing mice.

---

**Correspondence to:** Dr Te-Wei Lee, Institute of Nuclear Energy Research, No. 1000 Wenhua Rd., Jiaan Village, Longtan Township, Taoyuan County 32546, Taiwan, R.O.C.  
E-mail: twlee@iner.gov.tw

**Key words:** liposomes, Rhenium-188, therapeutic efficacy

## Materials and methods

**Materials.** The  $^{188}\text{W}/^{188}\text{Re}$  generator was purchased from Oak Ridge National Laboratory (Oak Ridge, USA). Elution of the  $^{188}\text{W}/^{188}\text{Re}$  generator with normal saline provided solutions of carrier-free  $^{188}\text{Re}$  as sodium perrhenate ( $\text{NaReO}_4$ ). The pegylated liposome (Nano-X) was provided by Taiwan Liposome Co. (Taipei, Taiwan). N,N-bis(2-mercaptoethyl)-N',N'-diethylethylenediamine (BMEDA) were purchased from ABX (Radeberg, Germany). Stannous chloride ( $\text{SnCl}_2$ ) was purchased from Merck (Darmstadt, Germany). Glucoheptonate powder and doxorubicin was purchased from Sigma-Aldrich Corp. (Bangalore, India). Sepharose CL-6B column were purchased from GE Healthcare (Uppsala, Sweden). All other chemicals were purchased from Merck. Dulbecco's modified Eagle's medium (DMEM) cell culture medium and fetal bovine serum (FBS) was purchased from Gibco (USA).

**Cell cultures and animal model.** The AR42J human pancreas carcinoma cell line was obtained from the American Type Culture Collection (Manassas, VA, USA). It was grown in Dulbecco's modified Eagle's medium (DMEM) medium supplemented with 10% (v/v) fetal bovine serum (FBS) and 2 mM L-glutamine at 37°C in 5%  $\text{CO}_2$ . Cells were detached with 0.05% trypsin/0.53 mM EDTA in Hanks' balanced salt solution (HBSS). Four-week-old male nude mice were obtained from the National Animal Center of Taiwan (Taipei, Taiwan), with food and water being provided *ad libitum* in the animal house of the INER. Animal protocols were approved by the Institutional Animal Care and Use Committee (IACUC) at the Institute of Nuclear Energy Research. Mice were subcutaneously inoculated with  $2 \times 10^6$  tumor cells in the right hind flank. Ten days after inoculation, the animals developed tumors of  $\sim 50$ – $100 \text{ mm}^3$  in size.

**Preparation of  $^{188}\text{Re}$ -(DXR)-liposome-BBN.** The method for radiolabeling BMEDA with  $^{188}\text{Re}$  was as previously described (15,16). The labeling efficiency of the  $^{188}\text{Re}$ -BMEDA complexes was checked by paper chromatography with normal saline as the eluent.  $^{188}\text{Re}$ -BMEDA was encapsulated in the liposomes using the ammonium sulfate gradient loading procedure, the labeling processes of  $^{188}\text{Re}$ -(DXR)-liposome-BBN were as follows. The pegylated nanoliposomes (0.5 ml), DSPE-PEG-BBN (5  $\mu\text{l}$ ; 40 mg/ml) with or without DXR (80  $\mu\text{l}$ ; 140 mg/ml) had added high specific activity  $^{188}\text{Re}$ -BMEDA (450–650 MBq per 0.5 ml) solution and incubation at 60°C for 30 min. The  $^{188}\text{Re}$ -liposome-BBN or  $^{188}\text{Re}$ -DXR-liposome-BBN was separated from free  $^{188}\text{Re}$ -BMEDA using sepharose CL-6B column (GE Healthcare) eluted with normal saline. The labeling efficiency of the pegylated nanoliposomes was determined using the activity in pegylated nanoliposomes or liposome-DXR-BBN after separation divided by the total activity before separation. The amount of doxorubicin trapped inside the liposome was analyzed.

**Calculation of the amount of bombesin molecules on the surface of liposomes.** The amount of bombesin on liposome solution was determined by BCA assay (bombesin molecules/ml liposome). The particle size and the number of phospholipid molecules per liposome can be measured by particle analyzer and phosphate

assay separately. The amount of particle per ml liposome solution can be calculated through the concentration of phospholipid and particle size of liposome (vesicles/ml liposome). Finally, the amount of bombesin molecules per vesicle through the amount of bombesin on liposome solution (bombesin molecules/ml liposome) and the amount of particle per ml liposome solution were calculated. In this experiment, the average amount of bombesin molecules on the surface of liposome is 511.

**MicroSPECT imaging and semi-quantification analysis of targeted  $^{188}\text{Re}$ -liposome-BBN.** Imaging was acquired using low-energy, high-resolution collimators at 1, 24, 48 and 72 h after intravenous injection of  $^{188}\text{Re}$ -liposome-BBN with or without cold BBN (2 mg/mouse). For imaging acquisition, the mice were anesthetized with 1–2% isoflurane in 100%  $\text{O}_2$ . The energy window was set at 155 keV  $\pm$  10–15%, the FOV (field of view) was 12.5 cm. SPECT imaging was followed by CT image acquisition (X-ray source: 50 kV, 0.4 mA; 256 projections) with the animal in exactly the same position. Images were calibrated to standardized uptake values (SUV) (15,20). For calculating standardised tumor uptake value (SUV), known radio activity  $\text{Re-}^{188}$  was performed as reference. The SUV was determined from the regions of interest (ROI) on the tumor with uptake. The SUV was calculated according to the following standard formula: measured activity concentration ( $\mu\text{Ci/g}$ )/[injected dose ( $\mu\text{Ci}$ )/body weight (g)]. The images revealed a high uptake in tumors at 1 and 24 h after intravenous injection.

**Therapeutic efficacy studies.** Nude mice were used and each was subcutaneously inoculated with AR42J cells ( $2 \times 10^6$ ) in the right hind flank. Approximately 10 days after inoculation, tumor-bearing mice were divided randomly into groups, 8–10 mice per group. The study was divided in two experiments: (A) combinational radio-chemotherapeutic efficacy of  $^{188}\text{Re}$ -(DXR)-liposome-BBN in AR42J tumor-bearing mouse model, (B) dose-dependent effect of radio-chemotherapeutic efficacy of  $^{188}\text{Re}$ -(DXR)-liposome-BBN in AR42J tumor-bearing mouse model. In every experiment, one group was randomly selected as the control. In study (A), 4 groups of mice were treated with  $^{188}\text{Re}$ -DXR-liposome-BBN (17.76 MBq/100  $\mu\text{l}$  of  $^{188}\text{Re}$ , 2 mg/kg DXR and 0.4  $\mu\text{mol}$  phospholipids),  $^{188}\text{Re}$ -liposome-BBN (17.76 MBq/100  $\mu\text{l}$  of  $^{188}\text{Re}$  and 0.4  $\mu\text{mol}$  phospholipids), Lipo-Dox-BBN (2 mg/kg DXR and 0.4  $\mu\text{mol}$  phospholipids) and normal saline by single i.v. injection, respectively. In study (B), 6 groups of mice were treated with  $^{188}\text{Re}$ -DXR-liposome-BBN (17.76 MBq/100  $\mu\text{l}$  of  $^{188}\text{Re}$ , 2 mg/kg DXR and average 3.7  $\mu\text{mol}$  phospholipids),  $^{188}\text{Re}$ -DXR-liposome-BBN (11.84 MBq/100  $\mu\text{l}$  of  $^{188}\text{Re}$ , 2 mg/kg DXR and average 3.7  $\mu\text{mol}$  phospholipids),  $^{188}\text{Re}$ -liposome-BBN (11.84 MBq/100  $\mu\text{l}$  of  $^{188}\text{Re}$  and average 3.7  $\mu\text{mol}$  phospholipids),  $^{188}\text{Re}$ -liposome-BBN (17.76 MBq/100  $\mu\text{l}$  of  $^{188}\text{Re}$  and average 3.7  $\mu\text{mol}$  phospholipids), Lipo-Dox-BBN (2 mg/kg DXR and average 3.7  $\mu\text{mol}$  phospholipids) and normal saline by single i.v. injection, respectively. Treatments were initiated when the volume of tumors was  $\sim 50$ – $100 \text{ mm}^3$ . The treatments were performed on day 0 as a single dose. Tumor was measured twice weekly by a digital calipers to document tumor growth. Tumor measurements were converted into tumor volume (V) using the formula (21,22):  $V = (Y \times W^2)/2$ ; where Y and W are the larger and smaller perpendicular diameters, respectively. All data are expressed as mean  $\pm$  standard deviation. The mean

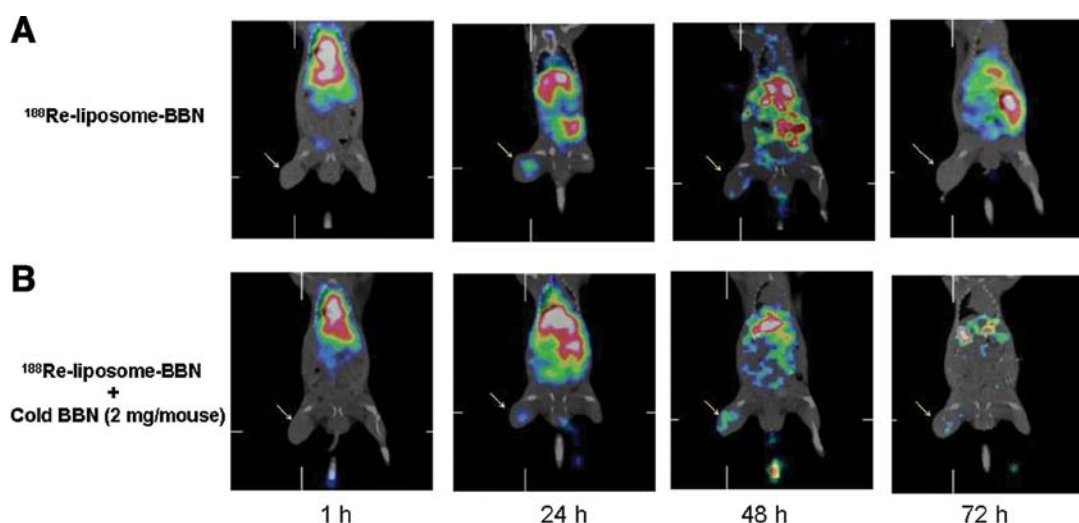


Figure 1. Comparisons of microSPECT/CT images of  $^{188}\text{Re}$ -liposome-BBN with or without cold BBN targeting AR42J tumors in nude mice. The coronal images were acquired at 1, 24, 48 and 72 h after injection of  $^{188}\text{Re}$ -liposome-BBN. The energy window was set at  $155 \text{ keV} \pm 10\text{-}15\%$ , the image size was set at  $64 \times 64$  pixel. (A) Images of mice of  $^{188}\text{Re}$ -liposome-BBN. (B) Images of mice of  $^{188}\text{Re}$ -liposome-BBN plus cold BBN (2 mg/mouse). The arrow marks the site of the tumor.

tumor growth inhibition rate (MGI) was calculated according to the volume of the tumor (23): growth rate of the treated group/growth rate of untreated group. Following standard animal-use protocols, termination was mandated on reaching one or both of the following criteria: a tumor weight of  $>2 \text{ g}$  (2 ml volume) or total body weight loss of  $>20\%$  (24). The combination therapeutic enhancement results were evaluated by the combination index (CI) (23,25). The CI expected growth inhibition rate/observed growth inhibition rate. The expected growth rate of combination treatment = tumor growth inhibition rate of drug A only  $\times$  tumor growth inhibition rate of drug B only. In this study, drug A is  $^{188}\text{Re}$ -DXR-liposome-BBN, and drug B is lipo-Dox-BBN. An index  $>1$  points to the synergistic effect, while that of  $<1$  indicates less than an additive effect.

## Results

**Labeling efficiency of  $^{188}\text{Re}$ -(DXR)-liposome-BBN.** The encapsulation efficiency of  $^{188}\text{Re}$ -BMEDA in pegylated liposome-BBN and liposome-BBN contain DXR was 54 and 76%, respectively. The radiochemical purity of  $^{188}\text{Re}$ -(DXR)-liposome-BBN was  $>95\%$ . The average particle size of  $^{188}\text{Re}$ -(DXR)-liposome ( $\sim 90 \text{ nm}$ ) was similar to the particle sizes before  $^{188}\text{Re}$ -BMEDA encapsulation.

**MicroSPECT/CT imaging of  $^{188}\text{Re}$ -liposome-BBN.** To confirm the specific targeting of the tumor sites of passive  $^{188}\text{Re}$ -liposome-BBN, microSPECT/CT imaging was performed. The microSPECT/CT imaging showed accumulated  $^{188}\text{Re}$ -liposome-BBN in the liver, spleen and tumor (Fig. 1A). The microSPECT/CT imaging of  $^{188}\text{Re}$ -liposome-BBN pointed to significant target and uptake in the tumors until 48 h after intravenous injection. The SUV of  $^{188}\text{Re}$ -liposome-BBN in tumor reach the peak at 24 h after injection ( $2.13 \pm 0.98$ ) (Table I). Contrary to microSPECT/CT imaging of  $^{188}\text{Re}$ -liposome-BBN with cold BBN (2 mg/mouse), the microSPECT/CT imaging showed significant decrease of  $^{188}\text{Re}$ -liposome-BBN uptake in the tumors at 24 h after injection (Fig. 1B).

Table I. The standardized uptake value (SUV) analysis of micro-SPECT/CT imaging of  $^{188}\text{Re}$ -liposome-BBN with or without cold BBN (2 mg/mouse) in AR42J tumor-bearing mouse model ( $n=3$ ).

Time (h)	$^{188}\text{Re}$ -liposome-BBN	$^{188}\text{Re}$ -liposome-BBN + cold BBN (2 mg/mouse)
1	$1.84 \pm 0.38$	$1.70 \pm 0.30$
24	$2.13 \pm 0.98$	$1.82 \pm 0.31$
48	$1.29 \pm 0.76$	$1.50 \pm 0.63$
72	$0.87 \pm 0.51$	$0.84 \pm 0.42$

**Therapeutic efficacy of  $^{188}\text{Re}$ -(DXR)-liposome-BBN.** In experiment (A) combinational radio-chemotherapeutic efficacy of  $^{188}\text{Re}$ -(DXR)-liposome-BBN in AR42J tumor-bearing mouse model, tumor volume growth and inhibition after various treatments from 0 to 23 days are plotted in Fig. 2A. In contrast to the mean tumor volume of  $1929 \pm 218 \text{ mm}^3$  in the untreated normal saline group at 19 d, the mean tumor volume of the treated groups at 19 d with  $^{188}\text{Re}$ -DXR-liposome-BBN (17.76 MBq, 2 mg/kg DXR),  $^{188}\text{Re}$ -liposome-BBN (17.76 MBq) and Lipo-Dox-BBN (2 mg/kg DXR) were  $178 \pm 42$ ,  $251 \pm 37$  and  $1284 \pm 144 \text{ mm}^3$ , respectively. As shown in Fig. 1A, the mean growth inhibition rates achieved by  $^{188}\text{Re}$ -DXR-liposome-BBN (17.76 MBq, 2 mg/kg DXR),  $^{188}\text{Re}$ -liposome-BBN (17.76 MBq) and Lipo-Dox-BBN (2 mg/kg DXR) were 0.092, 0.130 and 0.666, respectively. Significant additive tumor growth inhibition effect was demonstrated by the radiochemo-combination treatment with  $^{188}\text{Re}$ -DXR-liposome (CI 0.946; Table II).

In experiment (B) dose-dependent effect of radio-chemotherapeutic efficacy of  $^{188}\text{Re}$ -(DXR)-liposome-BBN in AR42J tumor-bearing mouse model, tumor volume growth and inhibition after various treatments from 0 to 26 days are plotted in Fig. 3A. In contrast to the mean tumor volume of  $2339 \pm 329 \text{ mm}^3$  in the untreated normal saline group at 18 d, the mean tumor volume

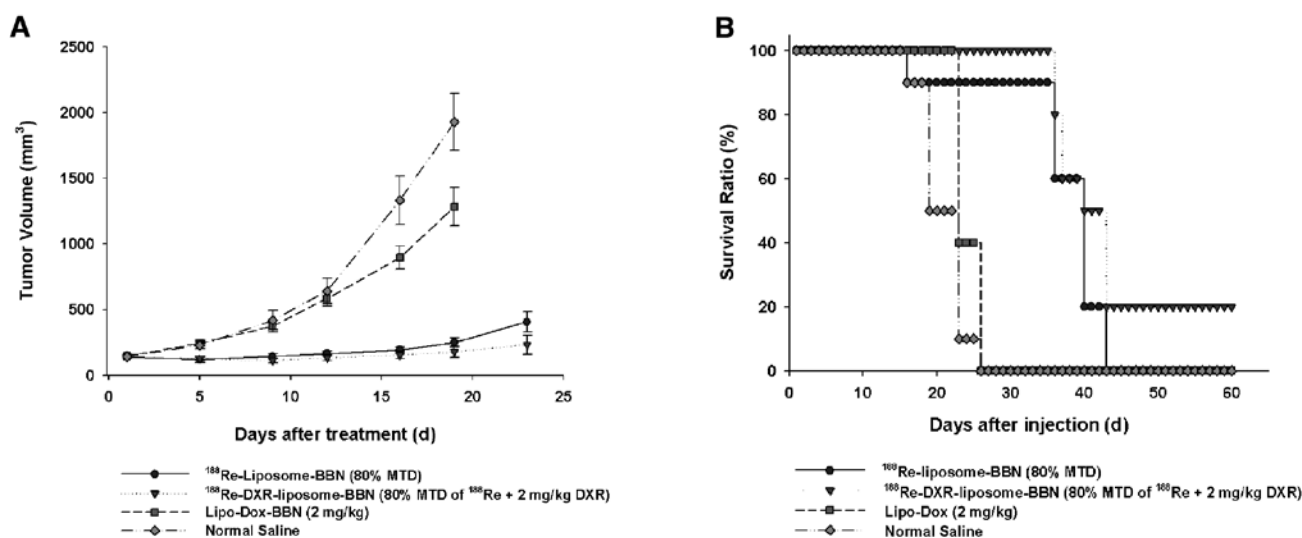


Figure 2. Tumor growth and survival curve. (A) Tumor growth volume ( $\text{mm}^3$ ) versus time (days) for nude mice implanted with AR42J tumors after administering  $^{188}\text{Re}$ -DXR-liposome-BBN (17.76 MBq of  $^{188}\text{Re}$ , 2 mg/kg DXR),  $^{188}\text{Re}$ -liposome-BBN (17.76 MBq of  $^{188}\text{Re}$ ), Lipo-Dox-BBN (2 mg/kg DXR) and normal saline by single i.v. injection on day 0. Tumor growth was significantly inhibited by the radiochemo-combination treatment of  $^{188}\text{Re}$ -DXR-liposome. (B) Survival curve for nude mice bearing AR42J tumors after i.v. injection of  $^{188}\text{Re}$ -DXR-liposome-BBN (17.76 MBq of  $^{188}\text{Re}$ , 2 mg/kg DXR),  $^{188}\text{Re}$ -liposome-BBN (17.76 MBq of  $^{188}\text{Re}$ ), Lipo-Dox-BBN (2 mg/kg DXR) and normal saline by single i.v. injection on day 0. Prolonged survival time and better survival rate of mice were observed after administration of radiochemo-bimodality  $^{188}\text{Re}$ -DXR-liposome-BBN. P-value for comparisons of survival curves of various treatment groups are listed in Table II.

Table II. The combinational radio-chemo therapeutic efficacy of  $^{188}\text{Re}$ -(DXR)-liposome-BBN in AR42J tumor-bearing mouse model.

Treatment modality	Tumor growth inhibition			Survival		
	MGI <sup>a</sup>	Expected <sup>b</sup>	CI <sup>c</sup>	Median survival time (d)	P-value <sup>d</sup>	Life span (%) <sup>e</sup>
$^{188}\text{Re}$ -liposomes-BBN	0.130			40.25	0.0002	+75.00
$^{188}\text{Re}$ -DXR-liposomes-BBN	0.092	0.087	0.946	43.00	0.0000	+86.96
Lipo-Dox-BBN (2 mg/kg)	0.666			23.83	0.0169	+3.61
Normal saline				23.00		

<sup>a</sup>MGI, mean growth inhibition rate = growth rate of treated group/growth rate of untreated group. <sup>b</sup>Expected growth inhibition rate = growth inhibition rate of  $^{188}\text{Re}$ -liposomes-BBN x growth inhibition rate of treatment of Lipo-Dox-BBN. <sup>c</sup>CI, combination index was calculated by dividing the expected growth inhibition rate by the observed growth inhibition rate. An index >0 indicates additive effect. <sup>d</sup>P-values were estimated by log-rank test,  $P < 0.05$  was considered statistically significant. <sup>e</sup>Percentage increase in life span was expressed as  $(T/C - 1) \times 100\%$ , where T is the median survival time of treated mice and C is the median survival time of control mice.

of the treated groups at 18 d with  $^{188}\text{Re}$ -DXR-liposome-BBN (17.76 MBq, 2 mg/kg DXR),  $^{188}\text{Re}$ -DXR-liposome-BBN (11.84 MBq, 2 mg/kg DXR),  $^{188}\text{Re}$ -liposome-BBN (11.84 MBq),  $^{188}\text{Re}$ -liposome-BBN (17.76 MBq) and Lipo-Dox-BBN (2 mg/kg DXR) were  $328 \pm 77$ ,  $457 \pm 52$ ,  $509 \pm 72$ ,  $414 \pm 77$  and  $1274 \pm 150 \text{ mm}^3$ , respectively. As shown in Fig. 2A, the mean growth inhibition rates achieved by  $^{188}\text{Re}$ -DXR-liposome-BBN (17.76 MBq, 2 mg/kg DXR),  $^{188}\text{Re}$ -DXR-liposome-BBN (11.84 MBq, 2 mg/kg DXR),  $^{188}\text{Re}$ -liposome-BBN (11.84 MBq),  $^{188}\text{Re}$ -liposome-BBN (17.76 MBq) and Lipo-Dox-BBN (2 mg/kg DXR) were 0.140, 0.198, 0.218, 0.177 and 0.545, respectively. Significant additive tumor growth inhibition effect was demonstrated by the radiochemo-combination treatment with  $^{188}\text{Re}$ -DXR-liposome (11.84 MBq, 2 mg/kg DXR) and  $^{188}\text{Re}$ -DXR-liposome (17.76 MBq, 2 mg/kg DXR) (CI 0.610 and 0.689, respectively; Table III).

In study (A), the survival curves for the different treatment groups are compared in Fig. 2B. The median survival time for the normal saline control mice was 23 d. The median survival times for the mice treated with  $^{188}\text{Re}$ -DXR-liposome-BBN (17.76 MBq, 2 mg/kg DXR),  $^{188}\text{Re}$ -liposome-BBN (17.76 MBq) and Lipo-Dox-BBN (2 mg/kg DXR) were 43.00 d ( $P < 0.05$ ), 40.25 d ( $P < 0.05$ ) and 23.83 d, respectively. The P-values for the differences among the survival curves of the various treatment groups are shown in Table II.

In study (B), the survival curves for the different treatment groups are compared in Fig. 3B. The median survival time for the normal saline control mice was 24 d. The median survival times for the mice treated with  $^{188}\text{Re}$ -DXR-liposome-BBN (17.76 MBq, 2 mg/kg DXR),  $^{188}\text{Re}$ -DXR-liposome-BBN (11.84 MBq, 2 mg/kg DXR),  $^{188}\text{Re}$ -liposome-BBN (11.84 MBq),  $^{188}\text{Re}$ -liposome-BBN (17.76 MBq) and Lipo-Dox-BBN (2 mg/kg DXR) were 43.00 d ( $P < 0.05$ ), 40.25 d ( $P < 0.05$ ) and 23.83 d, respectively. The P-values for the differences among the survival curves of the various treatment groups are shown in Table II.

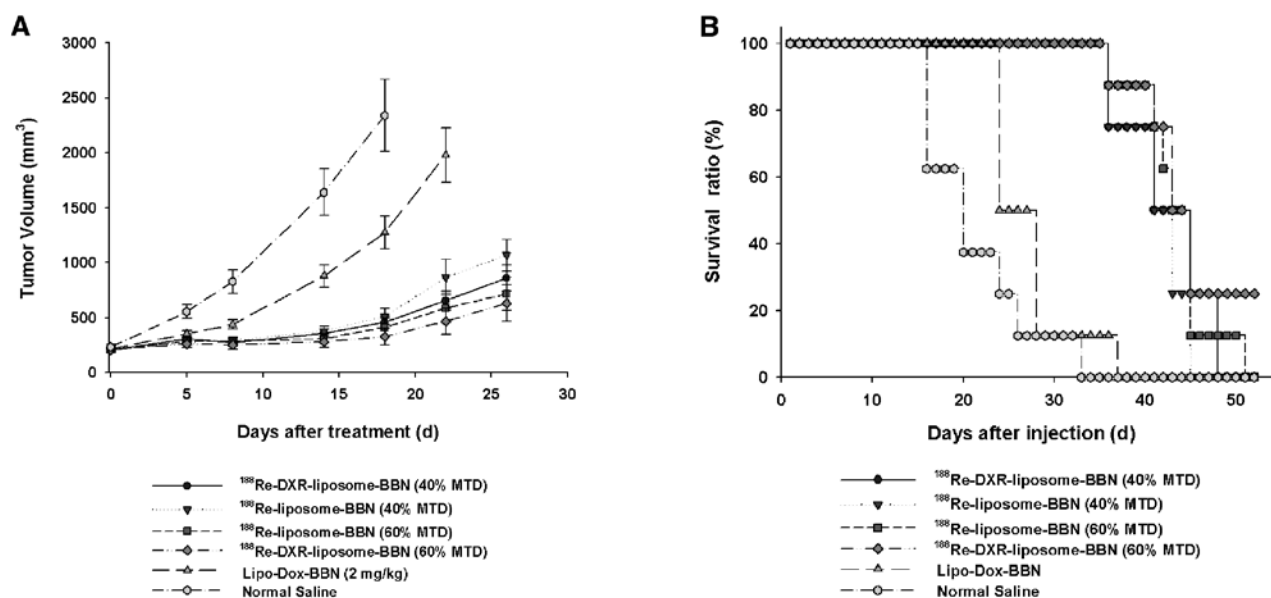


Figure 3. Tumor growth and survival curve. (A) Tumor growth volume (mm<sup>3</sup>) versus time (days) for nude mice implanted with AR42J tumors after administering <sup>188</sup>Re-DXR-liposome-BBN (17.76 MBq of <sup>188</sup>Re, 2 mg/kg DXR), <sup>188</sup>Re-DXR-liposome-BBN (11.84 MBq of <sup>188</sup>Re, 2 mg/kg DXR), <sup>188</sup>Re-liposome-BBN (11.84 MBq of <sup>188</sup>Re), <sup>188</sup>Re-liposome-BBN (17.76 MBq of <sup>188</sup>Re), Lipo-Dox-BBN (2 mg/kg DXR) and normal saline by single i.v. injection on day 0. Tumor growth was significantly inhibited by the highest dose radiochemo-combination treatment of <sup>188</sup>Re-DXR-liposome-BBN. (B) Survival curve for nude mice bearing AR42J tumors after i.v. injection of <sup>188</sup>Re-DXR-liposome-BBN (17.76 MBq of <sup>188</sup>Re, 2 mg/kg DXR), <sup>188</sup>Re-DXR-liposome-BBN (11.84 MBq of <sup>188</sup>Re, 2 mg/kg DXR), <sup>188</sup>Re-liposome-BBN (11.84 MBq of <sup>188</sup>Re), <sup>188</sup>Re-liposome-BBN (17.76 MBq of <sup>188</sup>Re), Lipo-Dox-BBN (2 mg/kg DXR) and normal saline by single i.v. injection on day 0. Prolonged survival time and better survival rate of mice were observed after administration of highest dose radiochemo-combination treatment of <sup>188</sup>Re-DXR-liposome-BBN. P-value for comparisons of survival curves of various treatment groups are listed in Table III.

Table III. The therapeutic efficacy of dose-dependent effect of radio-chemo therapeutic efficacy of <sup>188</sup>Re-(DXR)-liposome-BBN in AR42J tumor-bearing mouse model.

Treatment modality	Tumor growth inhibition			Survival		
	MGI <sup>a</sup>	Expected <sup>b</sup>	CI <sup>c</sup>	Median survival time (d)	P-value <sup>d</sup>	Life span (%) <sup>e</sup>
<sup>188</sup> Re-DXR-liposome-BBN (40% MTD)	0.195	0.119	0.610	43.50	0.0000	+81.25
<sup>188</sup> Re-DXR-liposome-BBN (60% MTD)	0.140	0.096	0.689	45.50	0.0000	+89.58
<sup>188</sup> Re-liposome-BBN (40% MTD)	0.218			30.33	0.0000	+26.37
<sup>188</sup> Re-liposome-BBN (60% MTD)	0.177			45.33	0.0000	+88.88
Lipo-Dox-BBN (2 mg/kg)	0.545			28.33	0.0578	+18.04
Normal saline				24.00	0.0000	

<sup>a</sup>MGI, mean growth inhibition rate = growth rate of treated group/growth rate of untreated group. <sup>b</sup>Expected growth inhibition rate = growth inhibition rate of <sup>188</sup>Re-liposomes-BBN x growth inhibition rate of treatment of Lipo-Dox-BBN. <sup>c</sup>CI, combination index was calculated by dividing the expected growth inhibition rate by the observed growth inhibition rate. An index >0 indicates additive effect. <sup>d</sup>P-values were estimated by log-rank test, P<0.05 was considered statistically significant. <sup>e</sup>Percentage increase in life span was expressed as (T/C - 1) x 100%, where T is the median survival time of treated mice and C is the median survival time of control mice.

kg DXR) were 45.50 d (P<0.05), 43.50 d (P<0.05), 30.33 d (P<0.05), 45.33 d (P<0.05) and 23.83 d, respectively. The P-values for the differences among the survival curves of the various treatment groups are shown in Table III.

## Discussion

The nuclear molecular imaging such as single photon emission computer tomography (SPECT) are valuable tools for new anti-

cancer drug discovery and development in preclinical animal models of human disease. In our previous studies, the results of biodistribution, pharmacokinetics and micro-SPECT/CT imaging demonstrated the benefits of passive radio-therapeutics of <sup>188</sup>Re-liposome in C26 colon carcinoma ascities, C26 colon solid tumor and HT-29 colon solid tumor animal models (15,16,20,26). In this study, the tumor targeting and therapeutic efficacy of bimodality radiochemo-combination treatment of <sup>188</sup>Re-(DXR)-liposome-BBN was investigated. The *in vivo*

microSPECT/CT imaging result of Fig. 1 displays AR42J tumor targeted by  $^{188}\text{Re}$ -liposomes-BBN, the decrease uptake of  $^{188}\text{Re}$ -liposome-BBN was shown after administration of cold BBN. These results indicated  $^{188}\text{Re}$ -liposome with BBN peptide targets the gastrin-releasing peptide receptors in the tumor.

The high energy  $\beta$  emitters of  $^{188}\text{Re}$  (2.12 MeV) have a mean tissue penetration range of 3.5 mm and maximum tissue penetration range of 10.15 mm (27,28), which enable  $^{188}\text{Re}$  to kill tumor cells through a cross-fire or non-specific cell killing effect. Li *et al* have studied the therapeutic efficacy of radioimmunotherapy (RIT) of  $^{188}\text{Re}$ -labeled herceptin, the tumor inhibition rate (IR) was  $48.8 \pm 4.9$  after the 4th week of  $^{188}\text{Re}$ -herceptin (11.1 MBq) administration by intravenous injection (29). Huang *et al* and Papahadjopoulos *et al* studied therapies of doxorubicin-encapsulating liposome in mice bearing C-26 colon carcinoma, the life span (%) of treatment with 3 and 10 mg/kg doxorubicin encapsulating liposome by triple injection was 1.3 and 5.1%, respectively (30,31). In this study, we use radiochemo-therapeutic  $^{188}\text{Re}$ -DXR-liposome-BBN for drug delivery to improve therapeutic efficacy and to reduce toxicity. In therapeutic experiment (A) and (B), the results (Table II) show dose-dependent anti-tumor activity of  $^{188}\text{Re}$ . The results (Table III) of comparisons of the therapeutic efficacy treatments with irradiation only (such as  $^{188}\text{Re}$ -liposome-BBN) or anti-tumor chemical drug only (such as Lipo-Dox-BBN) or dual radio-chemotherapy (such as  $^{188}\text{Re}$ -DXR-liposome-BBN) revealed that  $^{188}\text{Re}$ -DXR-liposome-BBN showed a better tumor growth inhibition rate, a higher survival ratio and life span of AR42J tumor-bearing mice treated with single doses (0.140, 45.50 d and 89.58%, respectively). The additive tumor regression effect of radiochemo-therapeutics of  $^{188}\text{Re}$ -DXR-liposome-BBN was also demonstrated in Table III.

Many effects have been demonstrated by conjugating various targeting ligands to the liposome surface to increase specificity of interaction of liposomal drugs with targeted cells and to enhance the amount of drugs delivered into tumor cells. Antibodies, peptides, growth factors and folate can selectively bind to target antigens or receptors overexpressed on the tumor cell. RGD-modified liposomes (32-34), integrin-targeted paclitaxel nanoparticles (35-38), and folate-conjugated liposomes (39) have been demonstrated to increase the intracellular delivery and therapeutic efficacy of chemotherapeutic agents *in vivo*. In our study, BBN targeted peptide conjugated with radio-chemotherapeutics  $^{188}\text{Re}$ -(DXR)-liposome was designed for treating solid pancreatic tumors by intravenous administration.

Apoptosis occurs spontaneously and is enhanced by irradiation. Radiation-induced apoptosis has been observed *in vivo* (40,41). Radiation-induced apoptosis is considered to be one of the main cell death mechanisms following exposure to irradiation. Apoptosis plays a modest role in the treatment response of most solid tumors, which constitute the main human malignancies. This is observed *in vivo* such as intestinal crypt, salivary and lacrimal glands with non-dividing cells, lymphocytes that are non-dividing, and is frequently seen early within 4-6 h after irradiation (40,42,43).  $^{188}\text{Re}$  kills tumor cells through a cross-fire or non-specific cell killing effect. Li *et al* have studied the therapeutic efficacy of radioimmunotherapy (RIT) of  $^{188}\text{Re}$ -labeled herceptin, the tumor inhibition rate (IR) was  $48.8 \pm 4.9$  after the 4th week of  $^{188}\text{Re}$ -herceptin (11.1 MBq) administration

by intravenous injection (29). Radiochemotherapeutics of  $^{188}\text{Re}$ -DXR-liposome attained significant survival time, ascites inhibition (decreased by 49 and 91% at 4 days after treatment;  $P < 0.05$ ) and tumor inhibition in mice (15,44). Radiotherapeutics with  $^{188}\text{Re}$ -liposomes provided better survival time (increased by 34.6% of life span;  $P < 0.05$ ), tumor and ascites inhibition (decreased by 63.4 and 83.3% at 7 days after treatment;  $P < 0.05$ ) in mice compared with chemotherapeutics of 5-fluorouracil (5-FU) (45). In conclusion, we used peptide targeted radiochemo-therapeutic multifunctional nanoliposome as carrier for drug delivery to improve therapeutic efficacy. The inhibition of tumor growth in mice treated with  $^{188}\text{Re}$ -DXR-liposome-BBN was precisely controlled and had longer survival time than those treated with anti-cancer drug,  $^{188}\text{Re}$ -liposome-BBN (MGI = 0.130; 75%), Lipo-Dox-BBN (MGI = 0.666; 3.61%) and untreated control mice. The additive tumor regression effect (Table II) was observed (CI 0.946) for co-delivery radiochemo-therapeutics of  $^{188}\text{Re}$ -DXR-liposome-BBN.

## Acknowledgements

The authors would like to thank Ching-Jun Liou for his help with the preparation of  $^{188}\text{Re}$ , and Cheng-Hui Chuang for her technical assistance in microSPECT/CT.

## References

- Allen TM: Ligand-targeted therapeutics in anticancer therapy. *Nat Rev Cancer* 2: 750-763, 2002.
- Maison W and Frangioni JV: Improved chemical strategies for the targeted therapy of cancer. *Angew Chem Int Ed Engl* 42: 4726-4728, 2003.
- Markwalder R and Reubi JC: Gastrin-releasing peptide receptors in the human prostate: relation to neoplastic transformation. *Cancer Res* 59: 1152-1159, 1999.
- Sun B, Halmos G, Schally AV, Wang X and Martinez M: Presence of receptors for bombesin/gastrin-releasing peptide and mRNA for three receptor subtypes in human prostate cancers. *Prostate* 42: 295-303, 2000.
- Gugger M and Reubi JC: Gastrin-releasing peptide receptors in non-neoplastic and neoplastic human breast. *Am J Pathol* 155: 2067-2076, 1999.
- Halmos G, Wittliff JL and Schally AV: Characterization of bombesin/gastrin-releasing peptide receptors in human breast cancer and their relationship to steroid receptor expression. *Cancer Res* 55: 280-287, 1995.
- Toi-Scott M, Jones CL and Kane MA: Clinical correlates of bombesin-like peptide receptor subtype expression in human lung cancer cells. *Lung Cancer* 15: 341-354, 1996.
- Minamino N, Kangawa K and Matsuo H: Neuromedin B: a novel bombesin-like peptide identified in porcine spinal cord. *Biochem Biophys Res Commun* 114: 541-548, 1983.
- McDonald TJ, Jornvall H, Tatemoto K and Mutt V: Identification and characterization of variant forms of the gastrin-releasing peptide (GRP). *FEBS Lett* 156: 349-356, 1983.
- Brannon-Peppas L and Blanchette JO: Nanoparticle and targeted systems for cancer therapy. *Adv Drug Deliv Rev* 56: 1649-1659, 2004.
- Allen TM and Cullis PR: Drug delivery systems: entering the mainstream. *Science* 303: 1818-1822, 2004.
- Torchilin VP: Recent advances with liposomes as pharmaceutical carriers. *Nat Rev Drug Discov* 4: 145-160, 2005.
- Newman MS, Colbern GT, Working PK, Engbers C and Amantea MA: Comparative pharmacokinetics, tissue distribution, and therapeutic effectiveness of cisplatin encapsulated in long-circulating, pegylated liposomes (SPI-077) in tumor-bearing mice. *Cancer Chemother Pharmacol* 43: 1-7, 1999.
- Vaage J, Donovan D, Wipff E, *et al*: Therapy of a xenografted human colonic carcinoma using cisplatin or doxorubicin encapsulated in long-circulating pegylated stealth liposomes. *Int J Cancer* 80: 134-137, 1999.



15. Chang YJ, Chang CH, Yu CY, *et al*: Therapeutic efficacy and microSPECT/CT imaging of  $^{188}\text{Re}$ -DXR-liposome in a C26 murine colon carcinoma solid tumor model. *Nucl Med Biol* 37: 95-104, 2010.
16. Chen MH, Chang CH, Chang YJ, *et al*: MicroSPECT/CT imaging and pharmacokinetics of  $^{188}\text{Re}$ -(DXR)-liposome in human colorectal adenocarcinoma-bearing mice. *Anticancer Res* 30: 65-72, 2010.
17. Emfietzoglou D, Kostarelos K and Sgouros G: An analytic dosimetry study for the use of radionuclide-liposome conjugates in internal radiotherapy. *J Nucl Med* 42: 499-504, 2001.
18. Ting G, Chang CH and Wang HE: Cancer nanotargeted radio-pharmaceuticals for tumor imaging and therapy. *Anticancer Res* 29: 4107-4118, 2009.
19. Ercan MT and Caglar M: Therapeutic radiopharmaceuticals. *Curr Pharm Des* 6: 1085-1121, 2000.
20. Chang YJ, Chang CH, Chang TJ, *et al*: Biodistribution, pharmacokinetics and microSPECT/CT imaging of  $^{188}\text{Re}$ -BMEDA-liposome in a C26 murine colon carcinoma solid tumor animal model. *Anticancer Res* 27: 2217-2225, 2007.
21. Carlsson G, Gullberg B and Hafstrom L: Estimation of liver tumor volume using different formulas - an experimental study in rats. *J Cancer Res Clin Oncol* 105: 20-23, 1983.
22. Fang F, Wang AP and Yang SF: Antitumor activity of a novel recombinant mutant human tumor necrosis factor-related apoptosis-inducing ligand. *Acta Pharmacol Sin* 26: 1373-1381, 2005.
23. Morgillo F, Kim WY, Kim ES, Ciardiello F, Hong WK and Lee HY: Implication of the insulin-like growth factor-IR pathway in the resistance of non-small cell lung cancer cells to treatment with gefitinib. *Clin Cancer Res* 13: 2795-2803, 2007.
24. Maddalena ME, Fox J, Chen J, *et al*:  $^{177}\text{Lu}$ -AMBA biodistribution, radiotherapeutic efficacy, imaging, and autoradiography in prostate cancer models with low GRP-R expression. *J Nucl Med* 50: 2017-2024, 2009.
25. Tan Y, Sun X, Xu M, *et al*: Efficacy of recombinant methioninase in combination with cisplatin on human colon tumors in nude mice. *Clin Cancer Res* 5: 2157-2163, 1999.
26. Chen LC, Chang CH, Yu CY, *et al*: Biodistribution, pharmacokinetics and imaging of  $^{188}\text{Re}$ -BMEDA-labeled pegylated liposomes after intraperitoneal injection in a C26 colon carcinoma ascites mouse model. *Nucl Med Biol* 34: 415-423, 2007.
27. Iznaga-Escobar N:  $^{188}\text{Re}$ -direct labeling of monoclonal antibodies for radioimmunotherapy of solid tumors: biodistribution, normal organ dosimetry, and toxicology. *Nucl Med Biol* 25: 441-447, 1998.
28. O'Donoghue JA, Bardies M and Wheldon TE: Relationships between tumor size and curability for uniformly targeted therapy with beta-emitting radionuclides. *J Nucl Med* 36: 1902-1909, 1995.
29. Li G, Wang Y, Huang K, Zhang H, Peng W and Zhang C: The experimental study on the radioimmunotherapy of the nasopharyngeal carcinoma overexpressing HER2/neu in nude mice model with intratumoral injection of  $^{188}\text{Re}$ -herceptin. *Nucl Med Biol* 32: 59-65, 2005.
30. Huang SK, Mayhew E, Gilani S, Lasic DD, Martin FJ and Papahadjopoulos D: Pharmacokinetics and therapeutics of sterically stabilized liposomes in mice bearing C-26 colon carcinoma. *Cancer Res* 52: 6774-6781, 1992.
31. Papahadjopoulos D, Allen TM, Gabizon A, *et al*: Sterically stabilized liposomes: improvements in pharmacokinetics and antitumor therapeutic efficacy. *Proc Natl Acad Sci USA* 88: 11460-11464, 1991.
32. Zhao H, Wang JC, Sun QS, Luo CL and Zhang Q: RGD-based strategies for improving antitumor activity of paclitaxel-loaded liposomes in nude mice xenografted with human ovarian cancer. *J Drug Target* 17: 10-18, 2009.
33. Xiong XB, Huang Y, Lu WL, *et al*: Enhanced intracellular delivery and improved antitumor efficacy of doxorubicin by sterically stabilized liposomes modified with a synthetic RGD mimetic. *J Control Release* 107: 262-275, 2005.
34. Xiong XB, Huang Y, Lu WL, *et al*: Intracellular delivery of doxorubicin with RGD-modified sterically stabilized liposomes for an improved antitumor efficacy: in vitro and in vivo. *J Pharm Sci* 94: 1782-1793, 2005.
35. Meng S, Su B, Li W, *et al*: Integrin-targeted paclitaxel nanoliposomes for tumor therapy. *Med Oncol* 28: 1180-1187, 2011.
36. Wartchow CA, Alters SE, Garzone PD, *et al*: Enhancement of the efficacy of an antagonist of an extracellular receptor by attachment to the surface of a biocompatible carrier. *Pharm Res* 21: 1880-1885, 2004.
37. Li L, Wartchow CA, Danthi SN, *et al*: A novel antiangiogenesis therapy using an integrin antagonist or anti-Flk-1 antibody coated  $^{90}\text{Y}$ -labeled nanoparticles. *Int J Radiat Oncol Biol Phys* 58: 1215-1227, 2004.
38. Du H, Cui C, Wang L, Liu H and Cui G: Novel tetrapeptide, RGDF, mediated tumor specific liposomal doxorubicin (DOX) preparations. *Mol Pharm* 8: 1224-1232, 2004.
39. Turk MJ, Waters DJ and Low PS: Folate-conjugated liposomes preferentially target macrophages associated with ovarian carcinoma. *Cancer Lett* 213: 165-172, 2004.
40. Milas L, Stephens LC and Meyn RE: Relation of apoptosis to cancer therapy. *In Vivo* 8: 665-673, 1994.
41. Meyn RE, Stephens LC, Hunter NR and Milas L: Apoptosis in murine tumors treated with chemotherapy agents. *Anticancer Drugs* 6: 443-450, 1995.
42. Cunningham D: Current status of colorectal cancer: CPT-11 (irinotecan), a therapeutic innovation. *Eur J Cancer* 32A (Suppl 3): S1-S8, 1996.
43. Chung KY and Saltz LB: Adjuvant therapy of colon cancer: current status and future directions. *Cancer J* 13: 192-197, 2007.
44. Chen LC, Chang CH, Yu CY, *et al*: Pharmacokinetics, micro-SPECT/CT imaging and therapeutic efficacy of  $^{188}\text{Re}$ -DXR-liposome in C26 colon carcinoma ascites mice model. *Nucl Med Biol* 35: 883-893, 2008.
45. Tsai CC, Chang CH, Chen LC, *et al*: Biodistribution and pharmacokinetics of  $^{188}\text{Re}$ -liposomes and their comparative therapeutic efficacy with 5-fluorouracil in C26 colonic peritoneal carcinoma mice. *Int J Nanomed* 6: 2607-2619, 2011.